



Short Communication

Achieving ultrafine-grained structure in a pure nickel by friction stir processing with additional cooling



P. Xue, B.L. Xiao, Z.Y. Ma*

Shenyang National Laboratory for Materials Science, Institute of Metal Research, Chinese Academy of Sciences, 72 Wenhua Road, Shenyang 110016, China

ARTICLE INFO

Article history:

Received 27 July 2013

Accepted 1 December 2013

Available online 6 December 2013

ABSTRACT

Pure Ni was successfully friction stir processed (FSP) using a common heat-treated steel tool under additional water cooling. The FSP Ni exhibited a multi-modal grain size distribution, with some relatively coarse grains of about 3–5 μm distributed in the ultra-fine grained (UFG) matrix. Sound tensile properties with a high yield strength of ~ 500 MPa and a large uniform elongation of $\sim 12\%$ were achieved in the UFG FSP Ni, attributable to the enhanced strain hardening capacity. This study describes an effective low-cost method of processing high melting point metals, and also provides a methodology to produce UFG pure Ni by FSP.

© 2013 Elsevier Ltd. All rights reserved.

1. Introduction

Since the invention, friction stir welding and processing (FSW/P) have been widely applied, especially in aerospace and automotive areas [1,2]. Initially, FSW/P were applied primarily to aluminum alloys, which can be easily welded and processed due to their low melting temperature and sound plastic deformation ability [1–4]. Other metals with relatively low melting points, such as copper and magnesium alloys, have been also subjected to wide FSW/P investigations [1,2,5,6]. By contrast, it was difficult to conduct FSW/P on ferrous metals and other high melting point metals, which was limited by the development of the welding tools [7–12].

During FSW/P, most of the heat generates from the severe friction between the rotation tool and the workpiece, and the maximum temperature in the stirred zone (SZ) is usually between $0.6T_m$ and $0.9T_m$, where T_m is the workpiece's melting point [1,13,14]. Therefore, during FSW/P of high melting point metals, tools that are strong and durable at higher temperatures (usually higher than 1000 °C) are necessary to guarantee the successful welding and processing. In this case, polycrystalline cubic boron nitride (PCBN) and tungsten-based alloys are usually chosen as the tool materials [7–12,15–18]. However, there are some obvious drawbacks for these tools, such as the high cost, the tool oxidation, abrasion and reaction with the workpiece at higher temperatures [7–12].

To date, there are still no appropriate tool materials that can stand up to meet the requirement of FSW/P of high melting point metals well [7,11,12]. If the process temperature is reduced greatly during FSW/P of high melting point metals, there will be more choices for the tool materials. At lower welding/processing

temperatures, tool abrasion and reaction with the workpiece would be significantly inhibited, and no Ar shielding gas is needed. More importantly, the common tool materials with low cost may be suitable in this case.

Previous studies have proved that employing additional cooling is an effective method of reducing the process temperature during FSW/P [19–26]. Via additional cooling, mechanical properties of the FSW joints could be obviously enhanced and an ultra-fine grained (UFG) structure was successfully achieved in the SZ after FSW/P. The FSP UFG structure is usually characterized by equiaxed recrystallized grains with a large fraction of high angle grain boundaries (HAGBs, misorientation angle $\geq 15^\circ$) and low density of dislocations [20–26]. This is quite different from most severe plastically deformed (SPD) UFG microstructures originating from the dislocation related mechanisms [27,28], and special mechanical properties can be achieved in FSP UFG materials [25,26,29,30]. UFG structure has been successfully achieved by FSP in Al, Mg and Cu alloys [20–26]; however, there are no related studies on FSP UFG high melting point metals till now. So it is worthwhile to investigate the possibility for obtaining UFG high melting point metals with good mechanical properties by FSP.

In this study, a typical high melting point metal – pure Ni was subjected to FSP using a tool made of common heat-treated tool steel under additional rapid cooling. The aim is to (a) investigate the availability of the common tool materials for FSW/P of high melting point metals under additional cooling and (b) understand the relationship between the microstructure and mechanical properties of the FSP UFG Ni.

2. Experimental procedures

Commercially pure Ni (99.98%) plate, 4 mm in thickness, 150 mm in length and 80 mm in width was used in this study,

* Corresponding author. Tel./fax: +86 24 83978908.

E-mail address: zyxia@imr.ac.cn (Z.Y. Ma).

and the rotation tool was made of common heat-treated tool steel (M42). For the FSP process, the pure Ni plate was first fixed underwater prior to FSP, and then the water was allowed to flow during FSP. Thus, rapid cooling of the FSP sample was achieved by the flowing water. FSP was performed at a rotation rate of 400 rpm and a traverse speed of 50 mm/min, using a tool with a shoulder 10 mm in diameter and a cylindrical threaded pin 4 mm in diameter and 1.8 mm in length. For comparison, a routine FSP process was also performed in air with the same FSP parameter.

Microstructural observations were conducted by optical microscopy (OM), electron backscatter diffraction (EBSD), transmission electron microscopy (TEM, FEI Tecnai G² 20) and scanning electron microscopy (SEM), complemented by energy-dispersive spectroscopy (EDS). EBSD scans were performed using an Oxford HKL Channel 5 system on a LEO Supra 35 FEG SEM with a step size of 100 nm.

The dog-bone-shaped tensile specimens with a gauge length of 5 mm, a width of 1.2 mm and a thickness of 0.6 mm were machined along the FSP direction from the SZ. Uniaxial tensile tests were conducted at an initial strain rate of $1 \times 10^{-3} \text{ s}^{-1}$. The fracture surface was examined using SEM.

3. Results and discussion

Under additional water cooling in the present study, defect-free pure Ni was successfully processed by FSP using the steel tool, and

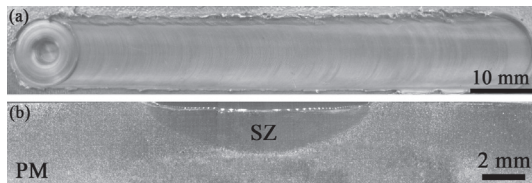


Fig. 1. (a) Surface macrograph and (b) cross-sectional macrostructure of FSP Ni sample prepared under additional water cooling.

no obvious tool abrasion was observed. Furthermore, no other elements besides Ni element were detected in the SZ according to the EDS results, indicating that the steel tool performed well in this case. However, when the FSP process was performed in air, the tool failed quickly after the shoulder touched the workpiece due to the greatly increased temperature. Fig. 1 shows the typical surface macrograph and the cross-sectional macrostructure of the FSP Ni sample prepared under additional water cooling. It is clear that sound processing surface was achieved and no defect was detected.

Obviously, additional cooling is an effective method of processing the high melting point metals, and this should be attributed to the greatly reduced process temperature. Most of the heat generated in the SZ was carried away by flowing water. Thus, the heat could not be accumulated during FSP, and therefore the process temperature was reduced greatly. In principle, FSW/P can be completed successfully using the steel tools and other low-cost tools at a lower processing temperature so long as the plastic flow of the materials runs well in the SZ. Fortunately, most metals, in particular the cubic system pure metals and alloys possess sound plastic deformation abilities even at a lower temperature. Therefore, this study provides an effective low-cost methodology to conduct FSW/P of high melting point metals.

From the EBSD image shown in Fig. 2a, the FSP Ni was characterized by an equiaxed recrystallized microstructure. However, the grain size exhibited a multi-modal distribution, with some relatively coarse grains of about 3–5 μm distributed in the UFG matrix. In the dynamic recrystallization (DRX) process during FSP, preferential grain growth might occur at the appropriate strain state, temperature, and misorientation, resulting in the wide grain size distribution [31]. This is different from the multi-modal UFG Ni prepared by cryomilling and quasi-isostatic (QI) forging processes, which originated from the nonuniformities of the cryomilled powders [32].

The distribution of the grain boundary misorientation angles of the FSP Ni is shown in Fig. 2b. Compared to the random distribution for a cubic polycrystal, the fraction of the low angle grain boundaries (LAGBs, misorientation angle $<15^\circ$) in the FSP Ni was

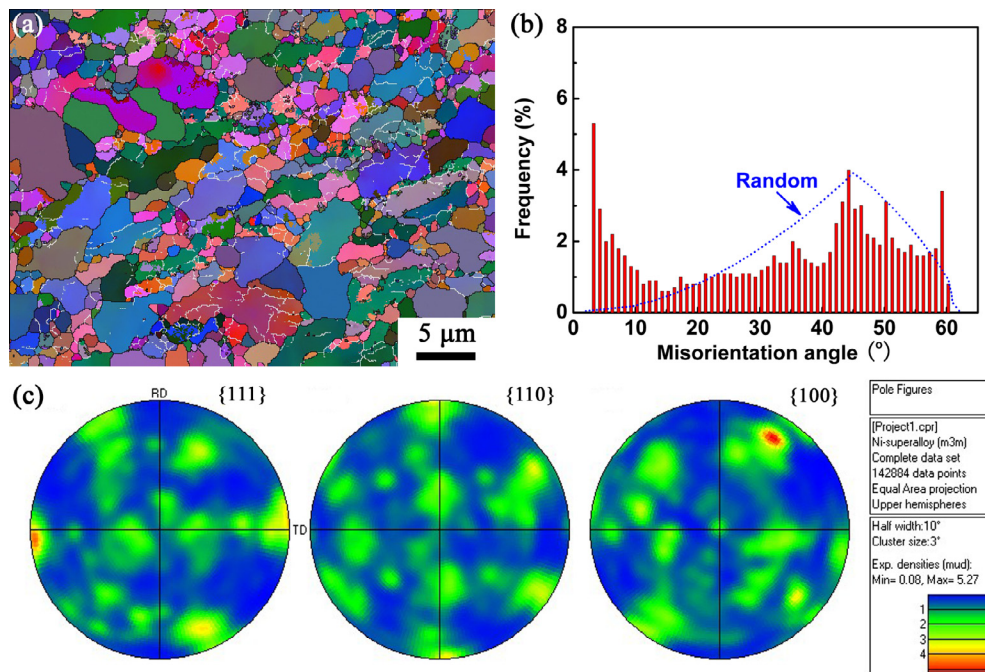


Fig. 2. Microstructure of FSP Ni: (a) EBSD image, HAGBs and LAGBs are represented by black and white lines, respectively, (b) grain boundary misorientation angle distribution, and (c) pole figures.

higher. This should be attributed to the ultra-fine subgrain structures in the FSP Ni, as shown by white lines in Fig. 2a. Considering all grain boundaries with misorientation angles $>2^\circ$, the HAGBs, in the FSP Ni comprised $\sim 80\%$ of the total grain boundary length, and this fraction was obviously larger than that in other SPD UFG materials [28,33].

Furthermore, it was revealed that the FSP Ni exhibited a weak texture component as indicated by the pole figures in Fig. 2c. This weak texture component was close to rotated cube orientation $\{001\} \langle 110 \rangle$, or so-called shear component, which came from the remnant of shear texture. The shear component was usually formed with inhomogeneous shear deformation due to the FSP. This result was similar to that of FSP Cu and Al alloys where very weak or random texture was found [34,35].

TEM examinations showed that the FSP Ni exhibited equiaxed UFG structure with a grain size of several hundred nanometers (Fig. 3). Besides the sharp, clear, and relatively straight boundaries which were identified as HAGBs, some wavy and ill-defined LAGBs were also observed, which was in accord with the EBSD result shown in Fig. 2a. This indicates that continuous DRX (CDRX) should happen in the FSP process, but the growth of the recrystallized grains was limited due to the rapid water cooling. Therefore, many dislocation structures or subgrain boundaries were preserved as shown in Figs. 2a and 3.

The tensile engineering stress–strain curves of the FSP Ni, as well as the coarse grained (CG) Ni reference material, are compared in Fig. 4. The CG Ni exhibited a low yield strength (YS) of about 100 MPa. It is apparent that the FSP Ni showed a high YS of about 500 MPa, which was higher than that of the multi-modal UFG Ni prepared by cryomilling and QI forging [32]. More importantly, the FSP Ni exhibited a considerable uniform elongation of $\sim 12\%$, suggesting that the fast plastic instability observed in most UFG materials [27,28] was restrained in the FSP Ni.

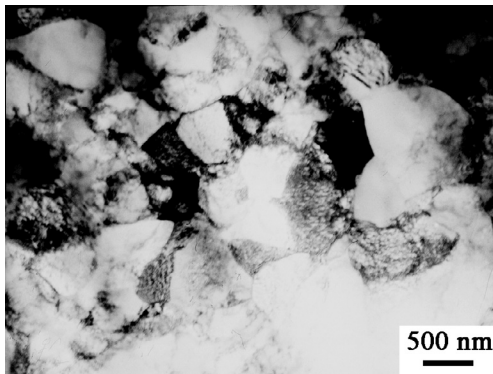


Fig. 3. Typical TEM bright-field image showing ultrafine grains in FSP Ni.

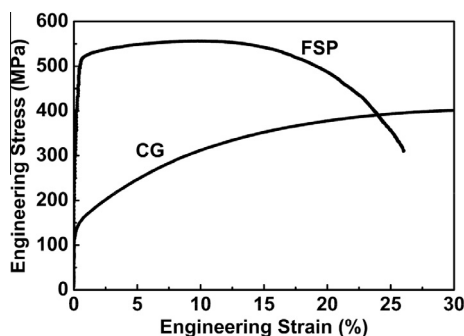


Fig. 4. Tensile engineering stress–strain curves of FSP Ni and CG Ni samples.

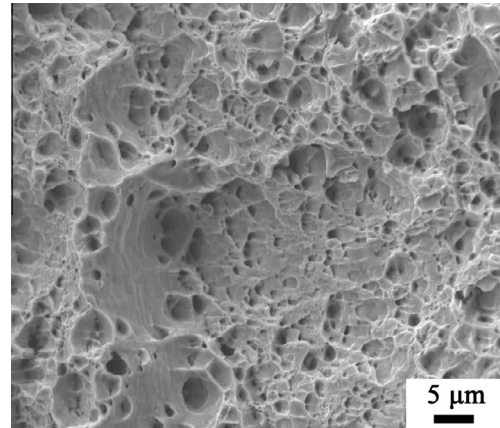


Fig. 5. SEM micrograph of the fracture surface of FSP Ni.

Fig. 5 shows the SEM micrograph of the fracture surface of the FSP Ni after the tensile test. The FSP Ni fractured with a ductile feature dominated by microvoid formation on a much finer scale. The refined grain/dislocation structures reduced the size of the nucleating flaws and increased the resistance to crack propagation, leading to a higher fracture stress.

The high ductility of the FSP Ni should be mainly attributed to the multi-modal grain size distribution. UFGs tend to lose the strain hardening quickly on deformation owing to their very low dislocation storage efficiency inside the tiny grains [27,28]. Such a high-strength material is therefore prone to plastic instability, severely limiting the desirable ductility. Previous studies indicated that multi-modal or bi-modal grain size distribution in UFG materials was beneficial to increasing the strain hardening capacity because the dislocation can be accumulated in the coarse grains [32,36]. In the present FSP Ni, a certain number of coarse grains existing in the UFG matrix, undoubtedly, would store dislocations effectively during tension, thereby enhancing strain hardening capacity.

Compared to other SPD UFG materials [28,33], one significant characteristic of the present FSP Ni is the large fraction of HAGBs (Fig. 2b). Though the mechanism for increasing strain hardening through the HAGBs is not fully understood, some studies showed that high fraction of HAGBs are beneficial to the strain hardening [32,37]. One possibility is that HAGBs are more effective in blocking slipping dislocations, thereby forcing the dislocations to tangle and accumulate near the boundaries. Another possible mechanism is by the occurrence of grain boundary sliding since sliding has been observed experimentally in UFG Al [38,39]. HAGB sliding leads to dislocation emissions at the triple junctions owing to the presence of high stress concentrations and these dislocations may act to increase the strain hardening. Anyhow, more dislocations can be accumulated in the special microstructures of the present FSP Ni, and enhanced strain hardening capacity was obtained, leading to the good combination of high strength and ductility.

From the above results, it is clear that high melting point pure Ni can be successfully friction stir processed using the tool made of common tool steel under additional water cooling. UFG Ni with a multi-modal structure was achieved and exhibited sound mechanical properties due to the special microstructure. This study describes an effective low-cost method of processing high melting point metals, and also provides a methodology to produce UFG pure Ni by FSP.

4. Conclusions

According to the above results and discussions, the following conclusions are reached:

- (1) Commercially pure Ni was successfully friction stir processed using the tool made of common tool steel under additional water cooling. The FSP Ni exhibited sound processing surface and no obvious tool abrasion was observed.
- (2) Defect-free UFG Ni was achieved in the SZ, which consisted of equiaxed recrystallized grains with a multi-modal grain size distribution, with some relatively coarse grains of about 3–5 μm distributed in the UFG matrix several hundred nanometers in grain size. The high fraction of the HAGBs of $\sim 80\%$ and a weak shear texture component were achieved in the FSP UFG Ni.
- (3) The FSP UFG Ni exhibited a good combination of strength and ductility, which showed a large uniform elongation of $\sim 12\%$ and a high YS of about 500 MPa. The sound tensile properties of the FSP Ni were attributed to the enhanced strain hardening in the special microstructure, where the dislocations could be accumulated effectively.

Acknowledgment

This work was supported by the National Natural Science Foundation of China under Grants Nos. 51071150 and 51331008.

References

- [1] Mishra RS, Ma ZY. Friction stir welding and processing. *Mater Sci Eng R* 2005;50(1–2):1–78.
- [2] Nandan R, DebRoy T, Bhadeshia HKDH. Recent advances in friction stir welding – Process, weldment structure and properties. *Prog Mater Sci* 2008;53(6):980–1023.
- [3] Cavaliere P, Cabibbo M, Panella F, Squillace A. 2198 Al–Li plates by friction stir welding: mechanical and microstructural behavior. *Mater Des* 2009;30(9):3622–31.
- [4] Sato YS, Park SHC, Kokawa H. Microstructural factors governing hardness in friction-stir welds of solid-solution-hardened Al alloys. *Metall Mater Trans A* 2001;32(12):3033–42.
- [5] Ni DR, Chen DL, Yang J, Ma ZY. Low cycle fatigue properties of friction stir welded joints of a semi-solid processed AZ91D magnesium alloy. *Mater Des* 2014;56:1–8.
- [6] Xue P, Xie GM, Xiao BL, Ma ZY, Geng L. Effect of heat input conditions on microstructure and mechanical properties of friction-stir-welded pure copper. *Metall Mater Trans A* 2010;41(8):2010–21.
- [7] Rai R, De A, Bhadeshia HKDH, DebRoy T. Review: friction stir welding tools. *Sci Tech Weld Join* 2011;16(4):325–42.
- [8] Thomas WM, Threadgill PL, Nicholas ED. Feasibility of friction stir welding steel. *Sci Technol Weld Join* 1999;4(6):365–72.
- [9] Collier M, Steel R, Nelson T, Sorensen C, Packer S. Grade development of polycrystalline cubic boron nitride for friction stir processing of ferrous alloys. *Mater Sci For* 2003;426–432(4):3011–6.
- [10] Meshram SD, Reddy GM, Pandey S. Friction stir welding of maraging steel (Grade-250). *Mater Des* 2013;49:58–64.
- [11] Bhadeshia H, DebRoy T. Critical assessment: friction stir welding of steels. *Sci Technol Weld Join* 2009;14(3):193–6.
- [12] Zhang YN, Cao X, Larose S, Wanjara P. Review of tools for friction stir welding and processing. *Can Metall Quart* 2012;51(3):250–61.
- [13] Sato YS, Urata M, Kokawa H. Parameters controlling microstructure and hardness during friction-stir welding of precipitation-hardenable aluminum alloy 6063. *Metall Mater Trans A* 2002;33(3):625–35.
- [14] Arbegast WJ, Hartley PJ. Friction stir weld technology development at Lockheed martin michoud space system- an overview. In: Proceedings of the fifth international conference on trends in welding research, Pine Mountain, GA, USA, June 1–5; 1998. p. 541–6.
- [15] Cho HH, Kang SH, Kim SH, Oh KH, Kim HJ, Chang WS, et al. Microstructural evolution in friction stir welding of high-strength linepipe steel. *Mater Des* 2012;34:258–67.
- [16] Reynolds AP, Tang W, Gnaupel-Herold T, Prask H. Structure, properties, and residual stress of 304L stainless steel friction stir welds. *Scr Mater* 2003;48(9):1289–94.
- [17] Sun YF, Fujii H, Takaki N, Okitsu Y. Microstructure and mechanical properties of mild steel joints prepared by a flat friction stir spot welding technique. *Mater Des* 2012;37:384–92.
- [18] Park SHC, Sato YS, Kokawa H, Okamoto K, Hirano S, Inagaki M. Rapid formation of the sigma phase in 304 stainless steel during friction stir welding. *Scr Mater* 2003;49(12):1175–80.
- [19] Xue P, Xiao BL, Zhang Q, Ma ZY. Achieving friction stir welded pure copper joints with nearly equal strength to parent metal via additional rapid cooling. *Scr Mater* 2011;64(11):1051–4.
- [20] Liu HJ, Zhang HJ, Yu L. Effect of welding speed on microstructures and mechanical properties of underwater friction stir welded 2219 aluminum alloy. *Mater Des* 2011;32(3):1548–53.
- [21] Su JQ, Nelson TW, Sterling CJ. Friction stir processing of large-area build UFG aluminum alloys. *Scr Mater* 2005;52(2):135–40.
- [22] Mofid MA, Abdollah-zadeh A, Ghaini FM. The effect of water cooling during dissimilar friction stir welding of Al alloy to Mg alloy. *Mater Des* 2012;36:161–7.
- [23] Chang CI, Du XH, Huang JC. Achieving ultrafine grain size in Mg–Al–Zn alloy by friction stir processing. *Scr Mater* 2007;57(3):209–12.
- [24] Morishige T, Hirata T, Tsujikawa M, Higashi K. Comprehensive analysis of minimum grain size in pure aluminum using friction stir processing. *Mater Lett* 2010;64(17):1905–8.
- [25] Xue P, Xiao BL, Ma ZY. High tensile ductility via enhanced strain hardening in ultrafine-grained Cu. *Mater Sci Eng A* 2012;532:106–10.
- [26] Xue P, Xiao BL, Ma ZY. Enhanced strength and ductility of friction stir processed Cu–Al alloys with abundant twin boundaries. *Scr Mater* 2013;68(9):751–4.
- [27] Dao M, Lu L, Asaro RJ, De Hosson JTM, Ma E. Toward a quantitative understanding of mechanical behavior of nanocrystalline metals. *Acta Mater* 2007;55(12):4041–65.
- [28] Zhilyaev AP, Langdon TG. Using high-pressure torsion for metal processing: Fundamentals and applications. *Prog Mater Sci* 2008;53(6):893–979.
- [29] Xue P, Xiao BL, Wang WG, Zhang Q, Wang D, Wang QZ, et al. Achieving ultrafine dual-phase structure with superior mechanical property in friction stir processed plain low carbon steel. *Mater Sci Eng A* 2013;575:30–4.
- [30] Xue P, Xiao BL, Ma ZY. Achieving large-area bulk ultrafine grained Cu via submerged multiple-pass friction stir processing. *J Mater Sci Technol* 2013;29(12):1111–5.
- [31] Doherty RD, Hughes DA, Humphreys FJ, Jonas JJ, Jensen DJ, Kassner ME, et al. Current issues in recrystallization: a review. *Mater Sci Eng A* 1997;238(2):219–74.
- [32] Zhao YH, Topping T, Bingert JF, Thornton JJ, Dangelewicz AM, Li Y, et al. High tensile ductility and strength in bulk nanostructured nickel. *Adv Mater* 2008;20(16):3028–33.
- [33] Huang CX, Yang HJ, Wu SD, Zhang ZF. Microstructural characterizations of Cu processed by ECAP from 4 to 24 passes. *Mater Sci Forum* 2008;584–586:333–7.
- [34] Liu FC, Ma ZY, Chen LQ. Low-temperature superplasticity of Al–Mg–Sc alloy produced by friction stir processing. *Scr Mater* 2009;60(11):968–71.
- [35] Oh-Ishi K, Zhilyaev AP, McNelley TR. A microtexture investigation of recrystallization during friction stir processing of as-cast NiAl bronze. *Metall Mater Trans A* 2006;37(7):2239–51.
- [36] Wang YM, Chen MW, Zhou FH, Ma E. High tensile ductility in a nanostructured metal. *Nature* 2002;419(6910):912–5.
- [37] Zhao YH, Zhu YT, Lavernia EJ. Strategies for improving tensile ductility of bulk nanostructured materials. *Adv Eng Mater* 2010;12(8):769–78.
- [38] Chinh NQ, Szommer P, Horita Z, Langdon TG. Experimental evidence for grain-boundary sliding in ultrafine-grained aluminum processed by severe plastic deformation. *Adv Mater* 2006;18(1):34–9.
- [39] Ivanov KV, Naydenkin EV. Grain boundary sliding in ultrafine grained aluminum under tension at room temperature. *Scr Mater* 2012;66(8):511–4.